

# LightMDETR: A Lightweight Approach for Low-Cost Open-Vocabulary Object Detection Training

Binta SOW<sup>1</sup>, Bilal FAYE<sup>2</sup>, Hanane AZZAG<sup>3</sup>, Mustapha Lebbah<sup>4</sup>

e-mail: bsow@aimsammi.org, faye@lipn.univ-paris13.fr, azzag@univ-paris13.fr, mustapha.lebbah@uvsq.fr

**Abstract**—Object detection in computer vision traditionally involves identifying objects in images. By integrating textual descriptions, we enhance this process, providing better context and accuracy. The MDETR model significantly advances this by combining image and text data for more versatile object detection and classification. However, MDETR’s complexity and high computational demands hinder its practical use. In this paper, we introduce Lightweight MDETR (LightMDETR), an optimized MDETR variant designed for improved computational efficiency while maintaining robust multimodal capabilities. Our approach involves freezing the MDETR backbone and training a sole component, the Deep Fusion Encoder (DFE), to represent image and text modalities. A learnable context vector enables the DFE to switch between these modalities. Evaluation on datasets like RefCOCO, RefCOCO+, and RefCOCOg demonstrates that LightMDETR achieves superior precision and accuracy.

## I. INTRODUCTION

Object detection is a key task in computer vision, involving identifying and localizing objects within images. Traditionally, closed-vocabulary models have been used, where models are trained to recognize a fixed set of object categories. Notable approaches like Faster R-CNN [1], YOLO [2], and SSD [3] have demonstrated high effectiveness but are limited in generalizing beyond predefined categories.

Open-vocabulary models offer new possibilities by using large, diverse datasets and unsupervised learning to detect objects not in the original training categories. Models like CLIP [4], ALIGN [5], and Florence [6] use transformer architectures to learn combined text and image representations, allowing for more flexible and context-sensitive object recognition.

In this context, open-vocabulary models like Multimodal Detr (MDETR) integrates image and text sequences, utilizing transformers to align visual and textual data for more versatile and accurate detection and classification. Similarly, Grounded Language-Image Pre-training (GLIP) [7] enhances detection performance by leveraging large-scale vision-language data. Models like RegionCLIP [8] and OWL-ViT [9] further advance multimodal learning by improving visual-textual alignment. These advancements highlight the potential of open-vocabulary models to revolutionize object detection, making it more adaptable to diverse and dynamic environments.

However, open-vocabulary models face significant challenges due to their complexity and high computational requirements, limiting their practical deployment in real-time applications or on resource-constrained devices.

To address these issues, we propose Lightweight MDETR (LightMDETR), an optimized version of the MDETR architecture. LightMDETR enhances computational efficiency while maintaining robust multimodal integration for object detection. Key optimizations include freezing the backbone components of the pre-trained model and introducing a “Deep Fusion Encoder” (DFE) to represent text and image modalities using shared parameters. By integrating learnable “context” parameters into each embedding, the DFE can effectively encode both modalities. This approach significantly reduces the number of parameters to tune while preserving the performance of the baseline MDETR model.

Our key contributions are summarized as follows:

- We introduce a lightweight method for open-vocabulary object detection that significantly reduces the number of parameters to tune, making training more cost-effective.
- We apply this approach to the MDETR architecture with two variants: LightMDETR, which trains only the “Deep Fusion Encoder” (DFE), and LightMDETR-CF, which extends LightMDETR with a cross-fusion layer between text and image modalities to enhance representation capability.
- We train only the DFE, freezing all pre-trained specialized backbone encoders for images and text. We achieve this by incorporating “context” parameters into the DFE, allowing it to switch between image and text modalities effectively.

## II. RELATED WORK

### A. Evolution of Object Detection: From Closed-Vocabulary to Open-Vocabulary Models

Object detection, a central task in computer vision, can be broadly categorized into closed-vocabulary and open-vocabulary methods.

**Closed-vocabulary object detection** focuses on detecting and classifying objects from a predefined, fixed set of categories. Notable models in this category include Faster R-CNN [1], which introduced the Region Proposal Network (RPN) to generate object proposals directly, making the process more efficient. YOLO [2] brought a novel approach by framing detection as a single regression problem, enabling real-time object detection by predicting bounding boxes and class probabilities in a single pass. SSD [3] improved detection accuracy, especially for small objects, by introducing multi-scale feature maps for predictions.

RetinaNet [10] addressed the challenge of class imbalance in object detection through its innovative Focal Loss, which down-weights the loss assigned to well-classified examples, enhancing the performance on hard-to-detect objects. Mask R-CNN [11] extended the Faster R-CNN framework by adding a parallel branch for predicting object masks, enabling instance segmentation in addition to object detection. While these models are highly effective within their defined scope, their limitation lies in their inability to generalize beyond the fixed set of classes, making them less adaptable in dynamic environments.

This limitation has paved the way for open-vocabulary object detection methods, driven by advances in models like CLIP [4].

**Open-vocabulary object detection** aims to transcend the constraints of fixed class categories by leveraging large-scale pretrained models that understand both text and image modalities. ViLD [12] uses CLIP’s embeddings to enable zero-shot object detection by matching image regions with any text description, a significant leap in flexibility and generalization. GLIP [7] integrates grounding into the pretraining process, allowing the model to learn the alignment between language and image regions more effectively. MDETR [13] combines textual cues dynamically with image features to improve detection in context-rich environments. Contextual Object Detection [14] emphasizes the role of surrounding context in improving detection accuracy, pushing the boundaries of what objects can be recognized by understanding relationships within the scene. Despite their superior generalization capabilities, these open-vocabulary methods are resource-intensive, requiring substantial computational power and large-scale datasets for training, primarily due to the reliance on extensive pretrained models for text and image encoding. Nonetheless, they represent a significant advancement in object detection, offering the ability to detect a vast range of objects, including those unseen during training.

To tackle the challenges associated with the extensive training required for open-vocabulary object detection, we propose a new method that significantly reduces training demands while maintaining performance. Our approach can be seamlessly integrated into any existing open-vocabulary object detection model, ensuring more efficient training without compromising the model’s effectiveness. *To demonstrate the effectiveness of our method, we validate it using the MDETR architecture.*

## B. MDETR: Modulated Detection for End-to-End Multi-Modal Understanding

MDETR advances object detection by integrating both visual and textual information into a unified framework. Unlike traditional object detection methods that classify objects into fixed categories, MDETR focuses on associating detected objects with spans of text tokens. The model uses ResNet [15] for visual feature extraction and RoBERTa [16] for textual feature extraction (ref. Figure 1). For training, MDETR employs two key loss functions to align image and

text data. The **soft token prediction loss** ( $\mathcal{L}_{soft.token}$ ) guides the model to predict a uniform distribution over the tokens in the text that correspond to each detected object, rather than predicting discrete class labels. Given a maximum token length  $L$  and a set of predicted bounding boxes, the loss for each object is computed by predicting the probability distribution over possible token positions. Specifically, if  $o_i$  represents the embedding of the  $i$ -th object and  $t_j$  denotes the  $j$ -th token, the soft token prediction loss is designed to minimize the discrepancy between predicted token spans and the true token spans in the text. The **contrastive alignment loss** enforces that the embeddings of visual objects and their corresponding text tokens are closely aligned in the feature space. This loss is calculated using:

$$\mathcal{L}_o = \frac{1}{N} \sum_{i=0}^{N-1} \frac{1}{|T_i^+|} \sum_{j \in T_i^+} -\log \left( \frac{\exp(o_i^\top t_j / \tau)}{\sum_{k=0}^{L-1} \exp(o_i^\top t_k / \tau)} \right) \quad (1)$$

$$\mathcal{L}_t = \frac{1}{L} \sum_{i=0}^{L-1} \frac{1}{|O_i^+|} \sum_{j \in O_i^+} -\log \left( \frac{\exp(t_i^\top o_j / \tau)}{\sum_{k=0}^{N-1} \exp(t_i^\top o_k / \tau)} \right) \quad (2)$$

where  $\tau$  is a temperature parameter set to 0.07,  $T_i^+$  is the set of tokens aligned with the  $i$ -th object, and  $O_i^+$  is the set of objects aligned with the  $i$ -th token. The total loss is the average of these two components:

$$\mathcal{L}_{contrast} = \frac{1}{2} (\mathcal{L}_o + \mathcal{L}_t) \quad (3)$$

The overall training loss for MDETR combines the bounding box losses (L1 and GIoU), soft token prediction loss, and contrastive alignment loss:

$$\mathcal{L}_{total} = \mathcal{L}_{bbox} + \mathcal{L}_{soft.token} + \mathcal{L}_{contrast} \quad (4)$$

with

$$\mathcal{L}_{bbox} = \mathcal{L}_{L1} + \mathcal{L}_{GIoU} \quad (5)$$

where  $\mathcal{L}_{L1}$  is the L1 loss calculated as:

$$\mathcal{L}_{L1} = \frac{1}{N} \sum_{i=1}^N \|\hat{b}_i - b_i\|_1 \quad (6)$$

and  $\mathcal{L}_{GIoU}$  is the Generalized Intersection over Union loss:

$$\mathcal{L}_{GIoU} = 1 - \text{IoU} + \frac{\text{area}(C - (A \cup B))}{\text{area}(C)} \quad (7)$$

where  $\hat{b}_i$  and  $b_i$  are the predicted and ground truth bounding boxes, respectively, and  $C$  is the smallest enclosing box covering both  $A$  and  $B$ .

Training the pretrained feature extractors ResNet and RoBERTa, as depicted in Figure 1, is both unnecessary and costly. To reduce training expenses while preserving MDETR’s performance, we propose a streamlined approach that involves freezing the pretrained ResNet and RoBERTa models and focusing on training a single component responsible for representing both image and text modalities.

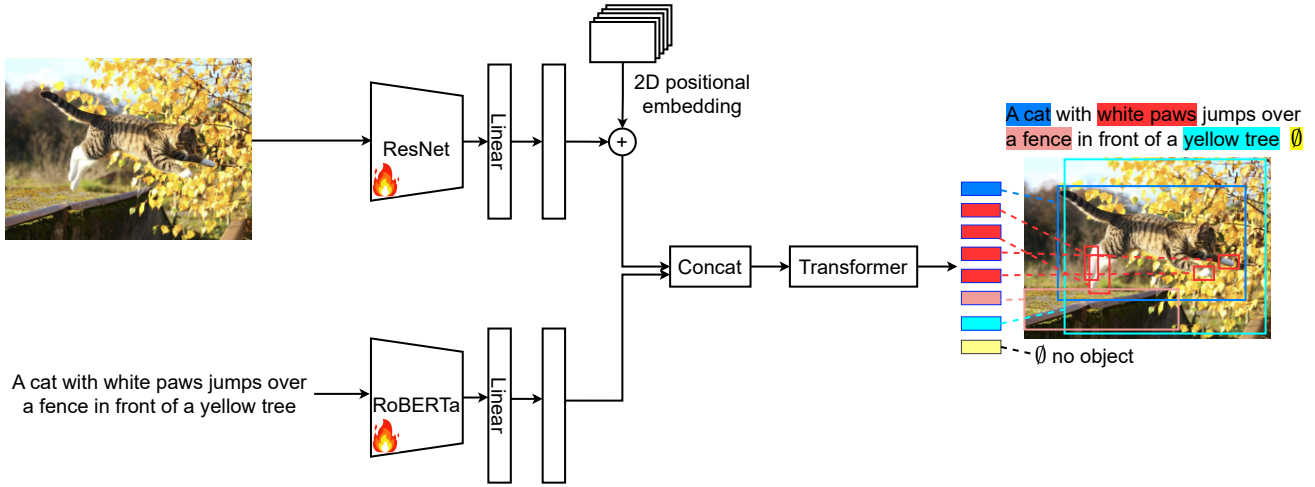


Fig. 1: MDETR Architecture: Visual features are extracted using ResNet, while textual features are extracted using RoBERTa.

### III. PROPOSED METHOD

Existing open-vocabulary object detection methods often rely on large, specialized pre-trained models to separately encode images and text—such as using ResNet for image encoding and RoBERTa for text encoding, as shown in Figure 1. Training these large models can be prohibitively expensive, which limits the practicality of open-vocabulary methods compared to their closed-vocabulary counterparts. To address this issue and reduce training costs while preserving performance, we propose a lightweight training approach. This method allows for cost-effective training of any open-vocabulary model without sacrificing performance. We validate our approach by applying it to MDETR, resulting in a new variant called LightMDETR (LightMDETR).

**LightMDETR** addresses the challenge of high training costs by freezing pre-trained feature extraction models, such as ResNet and RoBERTa, and introducing a single, lightweight component we developed called the “Deep Fusion Encoder” (DFE)  $f$ . The DFE integrates embeddings from both image and text encoders, streamlining the process while maintaining performance, as illustrated in Figure 2. To allow the DFE to encode inputs from different models, such as ResNet and RoBERTa, using the same parameters, a learnable context vector  $c_l$ , where  $l \in \{\text{image}, \text{text}\}$ , is fused with the embeddings. This approach enables the DFE to switch between image and text modalities while maintaining consistent parameter usage.

Consider  $O = \text{ResNet}(\text{image})$  as the output of a frozen ResNet for a given image and  $T = \text{RoBERTa}(\text{text})$  as the output of a frozen RoBERTa for the text description of that image. The DFE representation can be expressed as follows:

$$\begin{aligned} O_f &= f(O \otimes c_{\text{image}}) \\ T_f &= f(T \otimes c_{\text{text}}) \end{aligned} \quad (8)$$

where  $\otimes$  denotes the fusion operation (e.g., addition, multiplication, concatenation, or cross-attention), and  $c_{\text{image}}$

and  $c_{\text{text}}$  are randomly initialized vector parameters that match the dimensions of  $O_f$  and  $T_f$ , respectively. These vectors are learned as weights during the backpropagation process.

After the DFE processes the representations, the resulting features  $O$  and  $T$  are concatenated and fed into the DETR [17] “Transformer” (as shown in Figure 2). This enables the detection of relevant objects in the image, conditioned by the accompanying text.

To maintain a lightweight architecture, the DFE consists of two key components:

- A fusion block: which combines the context vector with the embeddings from the pretrained encoders.
- A single transformer layer: which refines and enhances the representation of the fused input, integrating both the embedding and context vector.

The loss function remains unchanged from MDETR (see Equation 4), allowing the learnable context vectors to be effectively adapted to the target task. This is achieved by directly contributing to the minimization of the loss function.

In MDETR, image and text features are encoded separately and only fused at the end before being input to the DETR. However, as noted in [18], effective phrase grounding in vision-language models requires early fusion of visual and textual features. To address this, we enhance LightMDETR by incorporating deep fusion of image and text features prior to DFE encoding, as illustrated in Figure 3. This modified approach is termed “Cross-Fusion LightMDETR” (LightMDETR-CF).

**LightMDETR-CF** incorporates three key components into LightMDETR: a cross-fusion layer featuring Multi-Head Attention (MHA) [19], and two additional transformer layers that refine the MHA outputs before they are fed into the DFE. The MHA mechanism takes as input the outputs of the ResNet and RoBERTa encoders, denoted as  $O$  and  $T$ , respectively. The transformations can then be expressed as

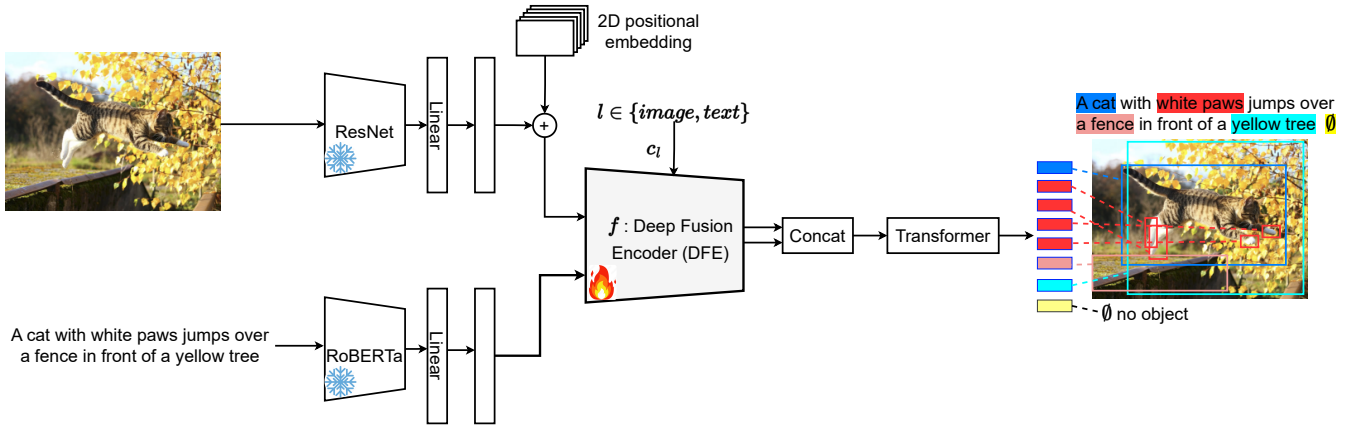


**Fig. 2:** LightMDETR architecture: ResNet and RoBERTa are frozen for feature extraction, with only the Deep Fusion Encoder (DFE)  $f$  being trained. A learnable context vector  $c_l$  where  $l \in \{\text{image, text}\}$ , is incorporated into the ResNet and RoBERTa embeddings, enabling the DFE to share parameters while switching between modalities. The rest of the architecture, including the “Transformer” module from DETR, remains unchanged from the baseline MDETR.

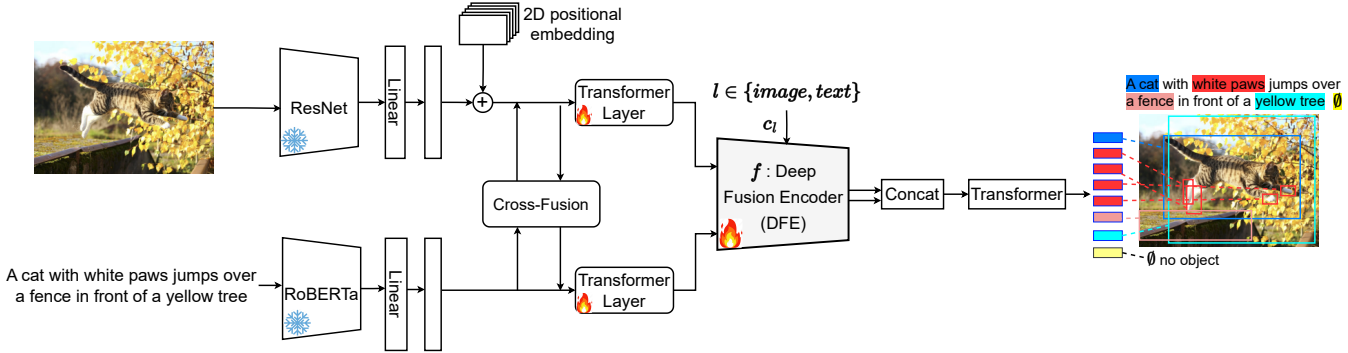


**Fig. 3:** Architecture of LightMDETR-CF: LightMDETR-CF extends LightMDETR 2 by introducing a cross-fusion layer prior to DFE encoding, thereby enhancing the model’s representation capabilities.

follows:

$$\begin{aligned}
 O^{(q)} &= OW^{(q,I)}, & T^{(q)} &= TW^{(q,T)}, & \text{Attn} &= \frac{O^{(q)} \cdot (T^{(q)})^\top}{\sqrt{d}}, \\
 T^{(v)} &= TW^{(v,T)}, & O_{\text{CF}} &= \text{SoftMax}(\text{Attn}) \cdot T^{(v)} \cdot W^{(\text{out},O)}, \\
 O^{(v)} &= OW^{(v,O)}, & T_{\text{CF}} &= \text{SoftMax}(\text{Attn}^\top) \cdot O^{(v)} \cdot W^{(\text{out},T)},
 \end{aligned} \tag{9}$$

where  $\{W^{(\text{symbol},O)}, W^{(\text{symbol},T)} : \text{symbol} \in \{q, v, \text{out}\}\}$  are trainable parameters that play similar roles to those of query, value, and output linear layers in MHA [19], respectively, and  $d$  corresponds the output dimension.

After applying the cross-fusion mechanism with the Multi-Head Attention approach, a projection is performed on  $O_{\text{CF}}$  and  $T_{\text{CF}}$  using two distinct Transformer layers:

$$\begin{aligned}
 O_{TL} &= \text{TransformerLayer}_O(O_{\text{CF}} + O), \\
 T_{TL} &= \text{TransformerLayer}_T(T_{\text{CF}} + T).
 \end{aligned} \tag{10}$$

The resulting  $O_{TL}$  and  $T_{TL}$  are then fed into the DFE, following a similar process as in LightMDETR, as described by:

$$\begin{aligned}
 O_f &= f(O_{TL} \otimes c_{\text{image}}), \\
 T_f &= f(T_{TL} \otimes c_{\text{text}}).
 \end{aligned} \tag{11}$$

These two approaches, LightMDETR and its variant LightMDETR-CF, provide an efficient strategy for training open-vocabulary object detection models. They significantly reduce training costs while maintaining high performance.

## IV. EXPERIMENT

### A. Pre-training

For the pre-training task, we adopt the MDETR approach, which leverages modulated detection to identify and detect all objects referenced in the corresponding free-form text.

For a fair comparison, we use the same combined training dataset as in [13], which integrates multiple image collections, including Flickr30k [20], MS COCO [21], and Visual Genome (VG) [22]. Flickr30k contains 31,783 images with detailed annotations for 158,915 region descriptions, primarily focused on objects and actions within the scenes. MS COCO contributes approximately 118,000 images, annotated with over 886,000 segmentations covering a wide range of common objects in diverse contexts. Visual Genome adds 108,077 images, with more than 5.4 million region descriptions and dense object annotations. For annotations, we leverage referring expressions datasets for fine-grained object references, VG regions for detailed

object-location relationships, Flickr entities for linking text descriptions with image regions, and the GQA train balanced set, which provides 1.7 million questions linked to object and scene graphs, enhancing the dataset’s ability to support complex reasoning tasks. This combined dataset ensures robust and comprehensive training, covering a diverse range of objects, contexts, and linguistic references.

For both the LightMDETR and LightMDETR-CF models, we use a frozen, pretrained RoBERTa-base [16] as the text encoder, which has 12 transformer layers, each with a hidden dimension of 768 and 12 attention heads, totaling 125M parameters. The visual backbone is a frozen, pretrained ResNet-101 [15], which has 44M parameters. By freezing both encoders, we reduce the trainable parameters in the backbone from 169 million in the original MDETR to zero in LightMDETR and LightMDETR-CF. Instead, the only trainable component in these models is the DFE (ref. Figure 2 and 3), which consists of a single transformer layer with 4 attention heads, amounting to 787,968 parameters to train. For the fusion operation in the DFE, as described in Equation 11, we use an addition method. The updated equations are:

$$\begin{aligned} O_f &= f(O + c_{\text{image}}) \\ T_f &= f(T + c_{\text{text}}) \end{aligned} \quad (12)$$

In these equations,  $c_{\text{image}}$  and  $c_{\text{text}}$  are initialized using a normal distribution and have the same dimension as  $O$  and  $T$ , which is 256.

All models undergo pre-training for 40 epochs with a substantial effective batch size of 64.

### B. Downstream Tasks

Models (LightMDETR and LightMDETR-CF) are evaluated in referring expression comprehension on RefCOCO [23], RefCOCO+ [24] and RefCOCOg [25] (ref. Table I. Referring expression comprehension involves the ability to accurately identify and localize objects in an image based on detailed natural language descriptions. This task requires interpreting the referring expressions—such as “the blue umbrella next to the park bench”—to extract specific attributes and spatial relationships. The goal is to map these textual descriptions to the corresponding objects in the image, ensuring precise object detection and localization by integrating both natural language processing and computer vision techniques.

Similar to MDETR, LightMDETR, and LightMDETR-CF are trained to predict bounding boxes for all objects mentioned in referring expressions, such as “blue umbrella” and “park bench.” However, the task in referring expression comprehension is to return a single bounding box corresponding to the object described by the entire expression. To address this, we fine-tune the model on a task-specific dataset for 5 epochs.

Table II presents a comparison of our models, LightMDETR and LightMDETR-CF, against other detection models on RefCOCO, RefCOCO+, and RefCOCOg. RefCOCO and

RefCOCO+ are evaluated using person vs. object splits: “testA” includes images with multiple people, while “testB” includes those with multiple objects. There is no overlap between training, validation, and testing images. RefCOCOg is split into two partitions.

Results presented in Table III showcase the precision performance of our models, LightMDETR and LightMDETR-CF, in comparison to MDETR on the RefCOCO, RefCOCO+, and RefCOCOg datasets. Precision at rank  $k$  (P@k) indicates the percentage of correct predictions within the top  $k$  ranked results. Specifically, P@1 measures precision at the top-1 prediction, P@5 within the top 5, and P@10 within the top 10.

Our models demonstrate competitive performance, with LightMDETR achieving the highest precision at P@1 on RefCOCO (85.92%) and RefCOCOg (80.97%), surpassing MDETR slightly on these datasets. Furthermore, LightMDETR-CF leads in P@5 on RefCOCO (95.52%) and P@10 on RefCOCOg (96.56%), highlighting the effectiveness of our lightweight approach. Although MDETR performs marginally better on RefCOCO+, LightMDETR closely follows, validating our hypothesis that freezing the backbone and training only the DFE component allows our models to achieve comparable, if not superior, performance with reduced computational complexity. This confirms the efficiency and accuracy of our proposed models in the referring expression comprehension task.

## V. CONCLUSION

We propose a novel method for training open-vocabulary object detection models that significantly reduces the number of parameters to tune. Our approach leverages specialized pretrained encoders for text and images, which remain frozen during training. The only component we train is a lightweight module we developed called the “Deep Fusion Encoder” (DFE). The DFE is designed to encode features from both the text and image encoders using shared parameters. To enable this, we introduce a learnable parameter called “context,” which identifies the source of each feature. This context is embedded in the DFE representation, allowing it to seamlessly switch between processing text and image features.

Our method, when integrated into the MDETR model, outperforms the baseline in terms of accuracy and precision on the referring expression comprehension tasks across the RefCOCO, RefCOCO+, and RefCOCOg datasets. Importantly, this approach is not limited to MDETR; it can be applied to any open-vocabulary object detection model to reduce training costs while maintaining high performance.

For future work, we plan to conduct further experiments to validate our method on tasks such as phrase grounding, referring expression segmentation, and visual question answering. Additionally, we will explore its application to other open-vocabulary object detection models.

Datasets	Images	Instances	Annotations	Categories	Image Size	Vocab. Size
RefCOCO	3,000	7,596	21,586	71	230 - 640	3,525
RefCOCO+	3,000	7,578	21,373	71	230 - 640	4,387
RefCOCOg	3,900	7,596	14,498	78	277 - 640	5,050

**TABLE I:** Datasets for validating referring expression comprehension.

Method	RefCOCO			RefCOCO+			RefCOCOg	
	val	testA	testB	val	testA	testB	val	test
MAttNet [26]	76.65	81.14	69.99	65.33	71.62	56.02	66.58	67.27
ViLBERT [27]	-	-	-	72.34	78.52	62.61	-	-
VL-BERT [28]	-	-	-	72.59	78.57	62.30	-	-
UNITER [29]	81.41	87.04	74.17	75.90	81.45	66.70	74.86	75.77
VILLA [30]	82.39	87.48	74.84	76.17	81.54	66.84	76.18	76.71
ERNIE-ViL [31]	-	-	-	75.95	82.07	66.88	-	-
MDETR	86.75	<b>89.58</b>	81.41	79.52	84.09	70.62	81.64	<b>80.89</b>
LightMDETR	86.77	88.50	<b>82.00</b>	<b>79.56</b>	83.28	70.60	<b>82.02</b>	79.67
LightMDETR-CF	<b>86.80</b>	88.76	81.78	79.10	<b>84.12</b>	<b>71.07</b>	81.06	80.81

**TABLE II:** Accuracy performance comparison between our proposed models, LightMDETR and LightMDETR-CF, and other detection models in the referring expression comprehension task on the RefCOCO, RefCOCO+, and RefCOCOg datasets. For testing, RefCOCO and RefCOCO+ datasets are evaluated using person vs. object splits: "testA" includes images with multiple people, while "testB" includes images with multiple objects from other categories. RefCOCOg features two distinct data partitions.

Method	RefCOCO			RefCOCO+			RefCOCOg		
	P@1	P@5	P@10	P@1	P@5	P@10	P@1	P@5	P@10
MDETR	85.90	95.41	96.67	<b>79.44</b>	<b>93.95</b>	<b>95.51</b>	80.88	94.19	95.97
LightMDETR	<b>85.92</b>	95.48	<b>96.76</b>	79.24	93.83	95.26	<b>80.97</b>	<b>94.87</b>	96.30
LightMDETR-CF	85.37	<b>95.52</b>	96.73	77.98	93.85	95.47	80.24	94.26	<b>96.56</b>

**TABLE III:** Precision performance comparison between our proposed models, LightMDETR and LightMDETR-CF, and MDETR in the referring expression comprehension task on the RefCOCO, RefCOCO+, and RefCOCOg datasets.

## REFERENCES

- [1] S. Ren, K. He, R. Girshick, and J. Sun, "Faster r-cnn: Towards real-time object detection with region proposal networks," *IEEE Transactions on Pattern Analysis and Machine Intelligence*, vol. 39, no. 6, pp. 1137–1149, 2015.
- [2] J. Redmon, S. Divvala, R. Girshick, and A. Farhadi, "You only look once: Unified, real-time object detection," in *Proceedings of the IEEE conference on computer vision and pattern recognition*, pp. 779–788, 2016.
- [3] W. Liu, D. Anguelov, D. Erhan, C. Szegedy, S. Reed, C.-Y. Fu, and A. C. Berg, "Ssd: Single shot multibox detector," in *European conference on computer vision*, pp. 21–37, Springer, 2016.
- [4] A. Radford, J. W. Kim, K. Hallacy, A. Ramesh, G. Goh, S. Agarwal, G. Sastry, A. Askell, P. Mishkin, J. Clark, *et al.*, "Learning transferable visual models from natural language supervision," in *International Conference on Machine Learning*, pp. 8748–8763, PMLR, 2021.
- [5] C. Jia, Y. Yang, Y. Xia, Y.-T. Chen, Z. Parekh, H. Pham, Q. V. Le, Y.-H. Sung, Z. Li, and T. Duerig, "Scaling up visual and vision-language representation learning with noisy text supervision," in *International Conference on Machine Learning*, pp. 4904–4916, PMLR, 2021.
- [6] L. Yuan, D. Chen, Y.-L. Chen, V. Codreanu, M. Guo, Y. Guo, L. He, H. H. Hu, Z. Hu, J. Liu, *et al.*, "Florence: A new foundation model for computer vision," *arXiv preprint arXiv:2111.11432*, 2021.
- [7] X. Li, X. Yin, C. Li, P. Zhang, X. Hu, L. Zhang, L. Wang, L. Li, M. Khabsa, C.-Y. Tsai, *et al.*, "Grounded language-image pre-training," *arXiv preprint arXiv:2205.11437*, 2022.
- [8] Y. Zhong, J. Chen, J. Li, C. Yuan, Z. Zheng, J. Wang, R. Ji, and T. Zhang, "Regionclip: Region-based language-image pretraining," *arXiv preprint arXiv:2112.09106*, 2022.
- [9] M. Minderer, Z. He, T. Chen, E. D. Cubuk, X. Zhai, and S. Mustikovela, "Simple open-vocabulary object detection with vision transformers," *arXiv preprint arXiv:2205.08547*, 2022.
- [10] T.-Y. Lin, P. Goyal, R. Girshick, K. He, and P. Dollár, "Focal loss for dense object detection," in *Proceedings of the IEEE international conference on computer vision*, pp. 2980–2988, 2017.
- [11] K. He, G. Gkioxari, P. Dollár, and R. Girshick, "Mask r-cnn," in *Proceedings of the IEEE International Conference on Computer Vision (ICCV)*, pp. 2961–2969, 2017.
- [12] X. Gu, T.-Y. Lin, W. Kuo, and Y. Cui, "Open-vocabulary object detection via vision and language knowledge distillation," *arXiv preprint arXiv:2104.13921*, 2021.
- [13] A. Kamath, M. Singh, Y. LeCun, G. Synnaeve, N. Carion, and I. Misra, "Mdetr-modulated detection for end-to-end multi-modal understanding," *arXiv preprint arXiv:2104.12763*, 2021.
- [14] Y. Zang, W. Li, J. Han, K. Zhou, and C. C. Loy, "Contextual object detection with multimodal large language models," *arXiv preprint arXiv:2305.18279*, 2023.
- [15] K. He, X. Zhang, S. Ren, and J. Sun, "Deep residual learning for image recognition," *IEEE Conference on Computer Vision and Pattern Recognition (CVPR)*, pp. 770–778, 2016.
- [16] Y. Liu, M. Ott, N. Goyal, J. Du, M. Zaheer, O. Levy, M. Lewis, L. Zettlemoyer, F. Shinn, R. Subba, and P. J. Liu, "Roberta: A robustly optimized bert pretraining approach," *arXiv preprint arXiv:1907.11692*, 2019.
- [17] N. Carion, F. Massa, G. Synnaeve, N. Usunier, A. Kirillov, and S. Zagoruyko, "End-to-end object detection with transformers," in *European conference on computer vision*, pp. 213–229, Springer, 2020.
- [18] J. Li, R. R. Selvaraju, A. D. Gotmare, S. Joty, C. Xiong, and S. Hoi, "Glip: Grounded language-image pre-training," in *Proceedings of the IEEE/CVF Conference on Computer Vision and Pattern Recognition*, 2022.
- [19] A. Vaswani, N. Shazeer, N. Parmar, J. Uszkoreit, L. Jones, A. N. Gomez, L. Kaiser, and I. Polosukhin, "Attention is all you need," in *Proceedings of the 31st International Conference on Neural Information Processing Systems (NeurIPS 2017)*, pp. 5998–6008, Curran Associates, Inc., 2017.
- [20] P. Young, A. Lai, M. Hodosh, and J. Hockenmaier, "From image descriptions to visual denotations: New similarity metrics for semantic inference over event descriptions," *Transactions of the Association for Computational Linguistics*, vol. 2, pp. 67–78, 2014.
- [21] T.-Y. Lin, M. Maire, S. Belongie, J. Hays, P. Perona, D. Ramanan, P. Dollár, and C. L. Zitnick, "Microsoft coco: Common objects in context," in *European conference on computer vision*, pp. 740–755, Springer, 2014.
- [22] R. Krishna, Y. Zhu, O. Groth, J. Johnson, K. Hata, J. Kravitz, S. Chen, Y. Kalantidis, L.-J. Li, D. A. Shamma, *et al.*, "Visual genome: Connecting language and vision using crowdsourced dense image

- annotations,” *International journal of computer vision*, vol. 123, no. 1, pp. 32–73, 2017.
- [23] A. Kazemzadeh, J. Hockenmaier, P. Young, L.-J. Li, and D. A. Shamma, “Referitgame: Referring to objects in photographs of real-world scenes,” in *Proceedings of the 2014 Conference on Empirical Methods in Natural Language Processing (EMNLP)*, pp. 786–795, 2014.
- [24] L. Yu, L.-J. Li, J. Hockenmaier, J. Deng, L. Zhang, X. Zhao, and Z. Tao, “Modeling context with deep neural networks for referring expression understanding,” in *Proceedings of the IEEE Conference on Computer Vision and Pattern Recognition (CVPR)*, pp. 1195–1204, 2016.
- [25] J. Mao, K. Xu, Y. Yang, and A. L. Yuille, “Generation and comprehension of unambiguous referring expressions,” in *Proceedings of the IEEE Conference on Computer Vision and Pattern Recognition (CVPR)*, pp. 11–20, 2016.
- [26] L. Yu, Z. Lin, X. Shen, J. Yang, X. Lu, M. Bansal, and T. L. Berg, “MATTNet: Modular attention network for referring expression comprehension,” in *Proceedings of the IEEE conference on computer vision and pattern recognition*, pp. 1307–1315, 2018.
- [27] J. Lu, D. Batra, D. Parikh, and S. Lee, “Vilbert: Pretraining task-agnostic visiolinguistic representations for vision-and-language tasks,” *Advances in neural information processing systems*, vol. 32, 2019.
- [28] W. Su, X. Zhu, Y. Cao, B. Li, L. Lu, and F. Wei, “Vl-bert: Pre-training of generic visual-linguistic representations,” in *International Conference on Learning Representations*, 2020.
- [29] Y.-C. Chen, L. Li, L. Yu, A. E. Kholy, F. Ahmed, Z. Gan, Y. Cheng, and J. Liu, “Uniter: Universal image-text representation learning,” in *European Conference on Computer Vision*, 2020.
- [30] Z. Gan, Y.-C. Chen, L. Li, C. Zhu, Y. Cheng, and J. Liu, “Large-scale adversarial training for vision-and-language representation learning,” *Advances in Neural Information Processing Systems*, vol. 33, pp. 6616–6628, 2020.
- [31] F. Yu, J. Tang, W. Yin, Y. Sun, H. Tian, H. Wu, and H. Wang, “Ernie-vil: Knowledge enhanced vision-language representations through scene graphs,” in *Proceedings of the AAAI conference on artificial intelligence*, vol. 35, pp. 3208–3216, 2021.